Rev. Real Acad. Cienc. Exactas Fis. Nat. Ser. A-Mat. (2024) 118:75
https://doi.org/10.1007/s13398-024-01578-z

ORIGINAL PAPER

A new paradigm in the logistic and similar maps: time stepping schemes

J. Alberto Conejero[1] · Òscar Garibo-i-Orts[2] · Carlos Lizama[3]

Received: 15 March 2023 / Accepted: 27 February 2024

Abstract
We propose the qualitative mathematical analysis of discrete models by replacing the classical Euler scheme of order 1 with Lubich quadrature time-stepping schemes. As the first study with this new paradigm, we compare the bifurcation diagrams for the logistic and sine maps obtained from discretizations of orders 1, 2, and 1/2.

Keywords Dynamical systems · Bifurcation diagrams · Logistic map · Sine map · Time-stepping schemes

Mathematics Subject Classification 65D32 · 65P20

1 Introduction

Since Verhulst's introduction of the logistic equation and later popularized by May, a great deal of research has been done from a mathematical and applied point of view. An essential task to understand this model's dynamics is to construct its bifurcation diagram. In fact, given an initial condition y_0, the iterations obtained through

$$y_{n+1} = \eta y_n(1 - y_n), \quad n \in \mathbb{N}_0, \tag{1}$$

show regimes of stability, periodicity, and chaos, depending on the values of the control parameter $\eta > 0$. It can be noted that after the change of variable $x_n = \frac{\eta}{\eta-1} y_n$ the equation

✉ J. Alberto Conejero
aconejero@upv.es

Òscar Garibo-i-Orts
oscar.garibo@campusviu.es

Carlos Lizama
carlos.lizama@usach.cl

[1] Instituto Universitario de Matemática Pura y Aplicada, Universitat Politècnica de València, Camí de Vera, s/n, 46022 València, Spain

[2] GRID-Grupo de Investigación en Ciencia de Datos, Valencian International University-VIU, Carrer Pintor Sorolla 21, 46002 València, Spain

[3] Departamento de Matemática y Ciencia de la Computación, Universidad de Santiago de Chile, Las Sophoras 173, Estación Central, Santiago, Chile

Published online: 23 March 2024

(1) is equivalent to

$$x_{n+1} - x_n = \mu x_n(1 - x_n) \tag{2}$$

where $\mu := \eta - 1$, see [1, 10]. Our key observation—and starting point—in this article is that the term $x_{n+1} - x_n$ represents a discretization of the first order derivative, say u', inherited from the continuous model

$$u'(t) = \mu f(u(t)), \quad t \geq 0, \tag{3}$$

where f is a given real-valued function. The discretization with step size one used on the left-hand side of (2) corresponds to what is commonly known as Euler's method in numerical analysis. From this observation, it is natural to ask:

(Q) *what happens if we change the Euler discretization method for another?*

In this work, we answer the previous question by proposing a new idea: we propose the problem

$$\sum_{j=0}^{n+1} b_{n+1-j} x_j = \mu f(x_n), \quad n \in \mathbb{N}_0, \tag{4}$$

where $(b_n)_n$ is a given sequence. To understand the consequences of this modification in the dynamics of discrete models, our objective of this article is twofold. First, to describe how to handle (4) by a methodology that uses inversion on its left side using a special convolution operator and, second, compare bifurcation diagrams of the associated dynamical systems for some representative cases.

It is worth noting that the left-hand side of (4) contains an important number of classical time-stepping schemes. For example, if we take $b_n = \delta_{0n} - \delta_{1n}$, where δ_{jn} denotes the Kronecker delta, we get (2) for $f(x) := x(1 - x)$.

From a numerical point of view, the sequences b_n are called quadrature weights. They arise from Lubich's quadrature methods [7], and we can determine them from the following generating power series (with step size $\tau = 1$)

$$G(\xi) = \sum_{n=0}^{\infty} b_n \xi^n, \tag{5}$$

named the symbol, or characteristic function, of the scheme [2].

For example for $G(\xi) = 1 - \xi$ we must have $b_n = \delta_{0n} - \delta_{1n}$, described previously. Other examples are the second order difference scheme which is given by the symbol $G(\xi) = (1 - \xi) + \frac{1}{2}(1 - \xi)^2$ (see [2]) and that produces $b_n = \frac{3}{2}\delta_{0n} - 2\delta_{1n} + \frac{1}{2}\delta_{2n}$; and the Euler scheme of order $1/2$ given by the symbol $G(\xi) = (1 - \xi)^{1/2}$ that produces $b_n = \frac{\Gamma(n-1/2)}{\Gamma(-1/2)n!}$. The first two cases are named local because they have a finite number of b_n different from zero. The third case is named non-local, and they usually incorporate memory effects in the model. For other examples, we refer to the works of Jin [2], Murillo-Arcila and Lizama [6] about maximal regularity of time-stepping schemes, the works of Wu and Baleanu that introduced a discrete version of the left Caputo differential operator [10, 11], and the work of Nieto for the solution of the logistic differential equation of fractional order without singular kernel [8, 13].

This article is organized as follows: In Sect. 2, we describe the general methodology that we follow to solve the problem (4), which allows it to be rewritten as an iterative equation of discrete convolutional type, with an explicit sequence kernel (as long as $b_0 \neq 0$). This procedure is exemplified in three dynamical systems, two local and one non-local, in the sense that the number of terms $b_n \neq 0$ is finite or infinite, respectively. As final observation,

we discussed about the possibility of studying the separation rate of nearby trajectories of the dynamical system (4).

In Sect. 3, we particularize the general setting described in Sect. 2 to the following cases: $f(x) = x(1-x)$ and $f(x) = \sin(x)$. We study graphically bifurcation diagrams.

Finally, in Sect. 4, we relate the equations obtained by means of the procedure indicated in Sect. 2, with models of viscoelasticity theory. This correspondence is found by means of the so called Poisson transformation, a method of discretization introduced in the reference [4]. For each model studied in the previous Sect. 3, the corresponding viscoelastic model is identified.

2 Methodology

In order to solve (4), we assume that there exists a sequence a_n such that $a_n * b_n = \delta_{0n}$ where $a_n * b_n = \sum_{j=0}^{n} a_{n-j} b_j$ denotes the convolution product between a_n and b_n and δ_{0n} is the Kronecker delta. Then, given x_0 and convolving with a_n in (4) we obtain

$$x_n = \mu \sum_{j=1}^{n} a_{n-j} f(x_{j-1}), \quad n \in \mathbb{N}. \tag{6}$$

Note that a_n always exists if $b_0 \neq 0$ and is given by the recurrence

$$a_0 = \frac{1}{b_0} \qquad a_n = -\frac{1}{b_0} \sum_{j=1}^{n} a_{n-j} b_j. \tag{7}$$

In other words, whenever $b_0 \neq 0$ we have that the convolution operator $K_b(x)_n := b_n * x_n$ that defines the left hand side in (4) has inverse K_a where a is defined as in (7). In fact, since clearly the convolution product is associative, we have

$$K_a(K_b(x))_n = a_n * K_b(x)_n = a_n * (b_n * x_n) = (a_n * b_n) * x_n = \delta_{0n} * x_n = x_n,$$

and analogously $K_b(K_b(x))_n = x_n$ because the convolution product is commutative. More generally, given any sequence b_n satisfying $b_0 \neq 0$ we have that K_b^{-1} exists and $K_b^{-1} = K_a$ where a_n satisfy the property $a_n * b_n = \delta_{0n}$, and is given explicitly by (7).

Using in (7) the sequences b_n obtained in the previous section, we have:

(a) For $b_n = \delta_{0n} - \delta_{1n}$ we obtain the constant sequence $a_n = 1$. Indeed, $b_0 = 1 \neq 0$ and $a_n * b_n = \sum_{j=0}^{n} a_{n-j} b_j = \sum_{j=0}^{n} b_j = \sum_{j=0}^{n} \delta_{0n} - \sum_{j=0}^{n} \delta_{1n} = 1$ for $n = 0$ and 0 otherwise. Moreover,

$$K_b(x)_n = \sum_{j=0}^{n} b_{n-j} x_j = x_n - x_{n-1}, \quad K_b^{-1}(x)_n = K_a(x)_n = \sum_{j=0}^{n} x_j.$$

(b) For $b_n = \frac{3}{2}\delta_{0n} - 2\delta_{1n} + \frac{1}{2}\delta_{2n}$ we obtain the sequence $a_n = 1 - \frac{1}{3^{n+1}}$, see [5, Example 4.2]. Moreover,

$$K_b(x)_n = \sum_{j=0}^{n} b_{n-j} x_j = \frac{3}{2} x_n - 2x_{n-1} + \frac{1}{2} x_{n-2}, \quad K_b^{-1}(x)_n = \sum_{j=0}^{n} \left(1 - \frac{1}{3^{n-j+1}}\right) x_j.$$

(c) For $b_n = \dfrac{\Gamma(n-1/2)}{\Gamma(-1/2)n!}$ we obtain the sequence $a_n = \dfrac{(2n)!}{4^n (n!)^2}$, see [5, Example 4.1]. The operator $K_b(x)$ and its inverse $K_b^{-1}(x)$ can be defined analogously.

Table 1 Euler approximation schemes of orders 1, 2 and 1/2, with the explicit formulas of the general solution

Scheme	General solution
(a) Euler (1st order)	$x_n = \mu \sum_{j=1}^{n} f(x_{n-1})$
(b) Euler (2nd order)	$x_n = \mu \sum_{j=1}^{n} \left(1 - \left(\frac{1}{3}\right)^{n-j+1}\right) f(x_{j-1})$
(c) Euler (1/2 order)	$x_n = \mu \sum_{j=1}^{n} \frac{(2(n-j))!}{4^{(n-j)}\,((n-j)!)^2} f(x_{j-1})$

Using (a), (b) and (c) above we obtain, respectively, the general schemes shown in Table 1

It is worth noting that from a qualitative point of view, the maximum Lyapunov exponent defined by

$$\sigma := \lim_{p\to\infty} \frac{1}{p} \sum_{j=1}^{p} \ln |f'(x_j)|, \tag{8}$$

where p is the period of an orbit x_i, plays a fundamental role in chaos theory. The maximum Lyapunov exponent measures the exponential rate of separation of nearby trajectories in a dynamical system, and it is used to determine the level of chaos in a system and provides information about its long-term predictability. A positive maximum Lyapunov exponent indicates chaotic behavior, while a negative exponent suggests stability.

We observe that the definition (8) depends on the left-hand side of (4). Specifically, the logarithm and the derivative have to do with the exponential nature of the solution to the linearized problem (Taylor series expansion):

$$u'(t) = f'(x)u(t), \tag{9}$$

where $x = u(t_0)$. For this reason, a plausible general equivalent of (8) in the discrete case (or even the continuous scenario) remains an open problem. For specific cases, for example fractional cases, a good assumption should have to do with the Mittag–Leffler function. We leave these considerations for a future article.

3 Results: bifurcation diagrams

For constructing the bifurcation diagrams, we consider pairs (x_0, μ), where x_0 is an initial condition and μ is taken in an interval where we want to illustrate the dynamics. For some diagrams presented in this work, we have taken several initial conditions, not only one, to improve the illustration of the dynamics. Given a pair (x_0, μ), we have computed the first 200 terms of each trajectory and represented the last 50 terms, namely $x_{151}, \ldots, x_{200}$. In Fig. 1, we have the bifurcation diagrams for first-order Euler models, $x_n = \mu \sum_{k=1}^{n} x_{k-1}(1 - x_{k-1})$ and $x_n = \mu \sum_{k=1}^{n} \sin(x_{k-1})$.

The first is the logistic map diagram; the second can also be found in [12]. We can observe that they are very similar since, as we have commented with the equivalences of (1) and (2), we can pass from one to the other one with a change of variable.

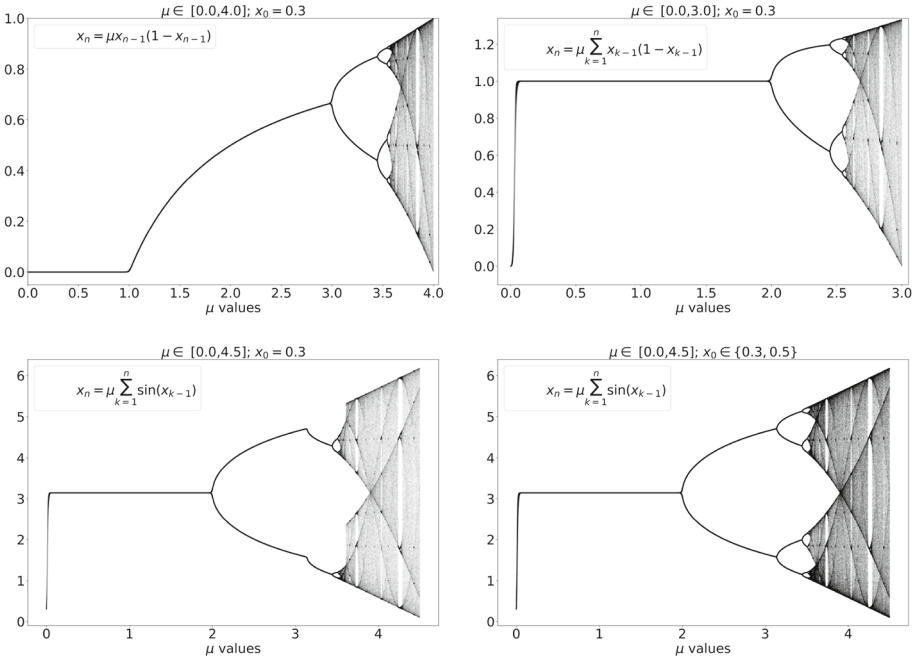

Fig. 1 Bifurcation diagrams for the logistic map (top left), the first-order logistic map (top right), and the first-order sine map for $x_0 = 0.3$ (bottom left) and $x_0 \in \{0.3, 0.5\}$ (bottom right). The μ step size is 10^{-4}

In order to avoid numerical precision problems in the computation of the bifurcation diagrams of second-order models, we have used the recurrent formula $x_n = \frac{2}{3}\left(2x_{n-1} - \frac{1}{2}x_{n-2} + \mu f(x_{n-1})\right)$ that directly appears from (4). Although a second-order model is numerically more stable than a first-order one, we can still find chaos in some regions, as shown in Fig. 2. We have simultaneously used several initial conditions to get better bifurcation diagram plots. For the case of the logistic term, we can find a chaotic region for $\mu \in [3.83, 3.85]$. Here, the step size for μ has been decreased up to 10^{-5}. For the sinus term, we show chaos in some regions of $\mu \in [6, 7]$ with a μ step size of 10^{-4}. For better plotting the behavior in the interval [6.18, 6.22] we have used 100 initial conditions, $x_0 \in \{0.01, 0.02, \ldots, 0.99\}$, computing the first 200 times of each trajectory, and plotting the last 25 terms of each one.

For the half-order case, where we have introduced the memory effect, the model resembles the fractional logistic models inspired by the fractional version of (2) [11], showing a blurry part in the region of chaos, as we can see in Fig. 3.

4 Analysis and conclusions

We have performed a comparative analysis of the dynamics exhibited by some time-stepping schemes originating from quadrature methods. From the recent literature, it is known that these methods are related to some linear viscoelasticity models. For instance, the Euler method is linked with a Newtonian fluid, the second order difference scheme is related to a Maxwell fluid, and the Euler scheme of order 1/2 with a power type material function,

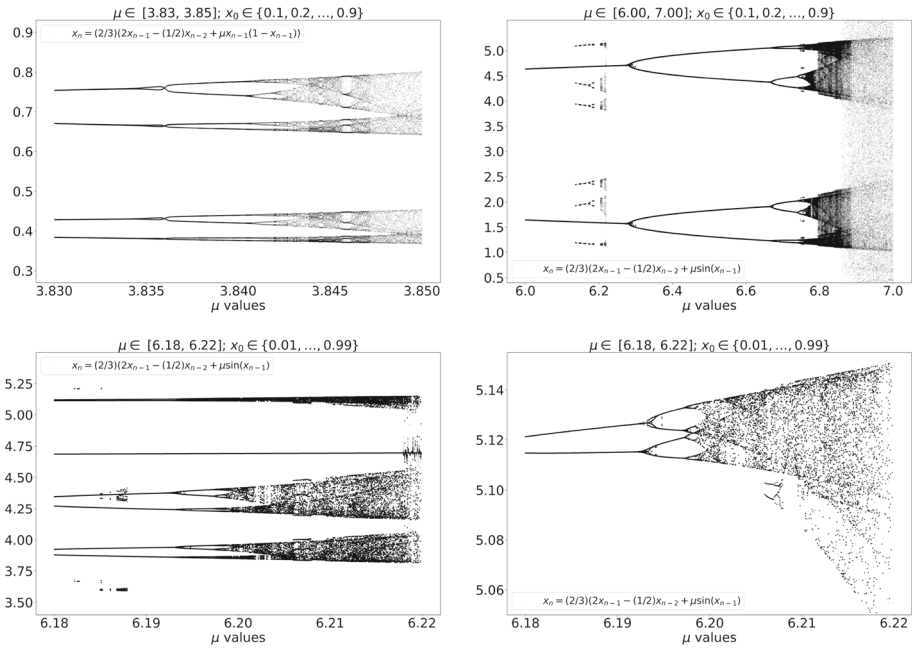

Fig. 2 Bifurcation diagrams for the second-order logistic map (top left) and for the second-order sine map (top right). In this second case, we can find smaller regions in the interval [6.18, 6.22] (bottom left and right)

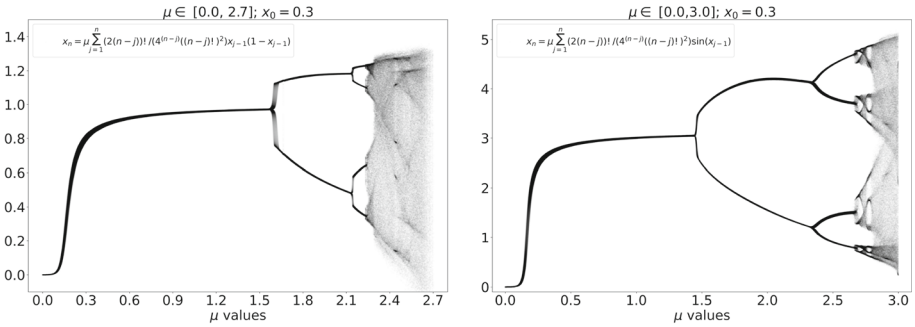

Fig. 3 Bifurcation diagrams for the half-order logistic map (left) and for the half-order sine map (right)

see [5]. On the other hand, from [9], it is well known that each one of the above-mentioned models has an associated material function. For instance, for a Newtonian fluid, the material function is $a(t) = 1$, for a Maxwell fluid $a(t) = 1 - e^{-ct}$ where $c \in \mathbb{R}$ is a constant, and for a power type material, the function is $a(t) = \frac{t^\alpha}{\Gamma(\alpha+1)}$ where $\alpha \in (0, 1)$, see [9, Section 5.2].

Now, we observe that each sequence a_n obtained for the time-stepping schemes in (6) corresponds in some sense to a discrete version of this material functions, namely, for $a(t) := 1$ we have $a_n = 1$; for $a(t) := 1 - e^{2t/3}$ we have $a_n = 1 - \frac{1}{3^{n+1}}$ and for $a(t) := \frac{t^{1/2}}{\Gamma(3/2)}$ we have $a_n = \frac{(2n)!}{4^n (n!)^2}$. We can even give a mathematical argument to prove this correspondence. For that, we consider the Poisson transformation [4] of a real-valued function $f : [0, \infty) \to \mathbb{R}$

Table 2 Comparative table of the numerical schemes and properties

Scheme	Viscoelastic model	Material function	Discrete kernel	Bifurcation diagram
Euler	Newtonian fluid	$a(t) = 1$	$a_n = 1$	Figure 1
Second order	Maxwell fluid	$a(t) = 1 - e^{-2t/3}$	$a_n = 1 - \frac{1}{3^{n+1}}$	Figure 2
Half order	Power type	$a(t) = \frac{t^{1/2}}{\Gamma(3/2)}$	$a_n = \frac{\Gamma(1/2+n)}{\Gamma(1/2)n!}$	Figure 3

defined by

$$\hat{f}(n) := \int_0^\infty p_n(t) f(t) dt, \quad n \in \mathbb{N},$$

where $p_n(t) = \frac{t^n}{n!} e^{-t}$ and note that a computation produces $\hat{a}(n) = 1 = a_n$, $\hat{a}(n) = 1 - \frac{1}{3^n} = a_{n-1}$ and $\hat{a}(n) = \frac{\Gamma(1/2+n)}{\Gamma(1/2)n!} = \frac{(2n)!}{4^n (n!)^2} = a_n$, respectively. We summarize the characteristic of the models and diagrams in Table 2.

In all cases, we have obtained explicit formulas for computing all the terms of the trajectory, as shown in Table 1. We have also shown the chaos phenomena in all these cases through bifurcation diagrams. In the models from half and first-order schemes, the bifurcation diagrams given by the logistic and sine functions present similar shapes, albeit with different parameter values. However, the similarities disappear when we observe the same maps with the second-order difference schemes. In these last cases, chaos is also present, but one has to look for small regions where it is present. Such dynamical systems show less chaotic behavior and are less powerful for encryption [3]. It will be interesting to study the dynamical properties of these dynamical systems and the connections with the physical properties of the associated viscoelastic models.

Acknowledgements JAC acknowledges funding from grant PID2021-124618NB-C21 funded by MCIN /AEI / 10.13039 /501100011033 and by "ERDF A way of making Europe", by the "European Union". CL is partially funded by ANID under FONDECYT grant number 1220036.

Data availability All data included in this article was synthetically generated from the formulas indicated in the text.

Declarations

Conflict of interest The authors declare no conflict of interest.

References

1. Conejero, J.A., Garibo-i Orts, Ò., Lizama, C.: Inferring the fractional nature of Wu–Baleanu trajectories. Nonlinear Dyn. **111**(13), 1–11 (2023)
2. Jin, B., Li, B., Zhou, Z.: Discrete maximal regularity of time-stepping schemes for fractional evolution equations. Numer. Math. (Heidelb.) **138**(1), 101–131 (2018)
3. Kumar, A., Alzabut, J., Kumari, S., Rani, M., Chugh, R.: Dynamical properties of a novel one dimensional chaotic map. Math. Biosci. Eng. **19**(3), 2489–2505 (2022)
4. Lizama, C.: The Poisson distribution, abstract fractional difference equations, and stability. Proc. Am. Math. Soc. **145**(9), 3809–3827 (2017)
5. Lizama, C., Murillo-Arcila, M.: Discrete maximal regularity for volterra equations and nonlocal time-stepping schemes. Discrete Contin. Dyn. Syst. Ser. A **40**(1), 509–528 (2020)
6. Lizama, C., Murillo-Arcila, M.: Maximal regularity for time-stepping schemes arising from convolution quadrature of non-local in time equations. Discrete Contin. Dyn. Syst. Ser. A **42**(8), 3787–3807 (2022)

7. Lubich, C.: Convolution quadrature and discretized operational calculus. I. Numer. Math. (Heidelb.) **52**(2), 129–145 (1988)
8. Nieto, J.J.: Solution of a fractional logistic ordinary differential equation. Appl. Math. Lett. **123**, 107568 (2022)
9. Prüss, J.: Evolutionary Integral Equations and Applications, vol. 87. Birkhäuser, Basel (2013)
10. Wu, G.C., Baleanu, D.: Discrete fractional logistic map and its chaos. Nonlinear Dyn. **75**(1–2), 283–287 (2014)
11. Wu, G.C., Baleanu, D.: Discrete chaos in fractional delayed logistic maps. Nonlinear Dyn. **80**(4), 1697–1703 (2015)
12. Wu, G.C., Baleanu, D., Zeng, S.D.: Discrete chaos in fractional sine and standard maps. Phys. Lett. A **378**(5–6), 484–487 (2014)
13. Zhang, T., Li, Y.: Exponential Euler scheme of multi-delay Caputo–Fabrizio fractional-order differential equations. Appl. Math. Lett. **124**, 107709 (2022)